Journal of Basic and Applied Engineering Research
Print ISSN: 2350-0077; Online ISSN: 2350-0255; Volume 1, Number 12; October-December 2014 pp. 153-157

http://www.krishisanskriti.org/jbaer.html

An Aerodynamic Analysis of Helli-net for Low Level Light Weight Radar (LLLR) using CFD

Gunjan Kumari[1], Utkarsh Agnihotri[2], Rajeev Jain[3], RK Sharma[4] and A.K. Saxena[5]

[1, 2,3,4,5]*Aerial Delivery Research and Development Establishment (ADRDE) Defence Research & Development Organisation, Post Box No. 51, Station Road, Agra -282 001, India*
E-mail: gunjan_kumari@adrde.drdo.in

Abstract: *This paper presents the external flow analysis of Helli-net for Low Level Light weight Radar (LLLR). Computational Fluid Dynamics (CFD) is used to compute the flow around a sharp-edged surface-mounted cube that resembles Helli-net with payload. A RANS (Reynolds Averaged Navier- Stokes) method is used for simulation to analyze flow separation, wake formation and flow behaviour around the body. Different visualization techniques of ANSYS FLUENT software are used, and the results of these are presented. Estimated aerodynamic data have been plotted to determine the trend. For given flight conditions, aerodynamic forces, flow patterns and aerodynamic coefficients for five different load conditions of Helli-net are analyzed.*

NOMENCLATURE

LLLR	=	*Low Level Light weight Radar*
EMRU	=	*Emergency Release Unit*
2D	=	*Two dimensional*
3D	=	*Three dimensional*
CFD	=	*Computational Fluid Dynamics*
Deg	=	*Degree*
MPa	=	*Mega Pascal*
K	=	*Kelvin*
mm	=	*millimeter*
m	=	*meter*
s	=	*second*
m/s	=	*meter per second*
Kg	=	*Kilogram*
C_D	=	*Coefficient of Drag*
C_L	=	*Coefficient of Lift*
C_l	=	*Coefficient of Rolling moment*
C_m	=	*Coefficient of Pitching moment*
C_n	=	*Coefficient of Yawing moment*
C_X	=	*Force coefficient in X direction*
C_Y	=	*Force coefficient in Y direction*
C_Z	=	*Force coefficient in Z direction*
α	=	*Angle of attack*
F_X	=	*Force in X direction*
F_Y	=	*Force in Y direction*
F_Z	=	*Force in Z direction*
L	=	*Reference Length*
A	=	Reference area

1. INTRODUCTION

Helli-net is designed for transportation of Low Level Light weight Radar (LLLR) for Helicopters.Helli-net is worked as an under-slung carrier.Helli-net also can be used for carrying supply items such as food, clothing, water, fuel; load of any irregular shape etc. under slung the Helicopter. Military uses Helli-net during immediate rescue/relief operations.LLLR / Supplies are kept in stacked packages in the Helli-net. Fig. 1 shows 3D CATIA model of assembled view of Helli-net with payload. Payload capacity is around 250 kg.

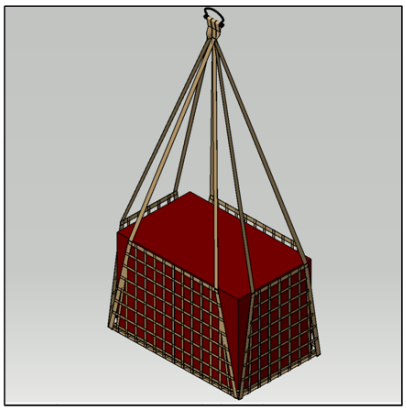

Fig. 1: CATIA 3D model of Heli-net for LLLR with payload

2. GEOMETRICALDESCRIPTION & 3D MODELING OF HELLI-NET

Helli-net is made of a textile net along with a D/clamp shackle. Basic material of Helli-net is nylon tape with thread sewing as per the IS standard used by designer. The D/clamp shackle acts as a coupling device between Cheetah helicopter and the Helli-net. The packed boxes of LLLR will be kept in the Helli-net. The four arms of the net will then be connected to the above mentioned shackle with help of four pulleys at one side.The other side of this shackle will be connected to the helicopter with the help of an anchoring wire rope, which is

part of helicopter.For different load conditions, stacked packages have been made. The overall dimension of this stacked packages are the outer body surface for CFD analysis. The thickness of tape used for net is very less in comparison to dimensions of payload. So, aerodynamic contribution of net will be very negligible in compare to payload. For simplification of problem, a rectangular box of respective payload dimensions is used for CFD analysis.

ICEM software is used for generating mesh for respective payloads. Fig. 2shows the extracted fluid domain of the Helli-net which has been used for meshing the CFD domain. An unstructured 3D tetrahedral mesh cells is generated as shown in Fig. 3.This tetrahedral mesh is converted to polyhedral mesh in FLUENT software used as a solver. By doing this overall mesh size gets reduced. Mesh is clustered near the wall of payload to capture the physics of flow.

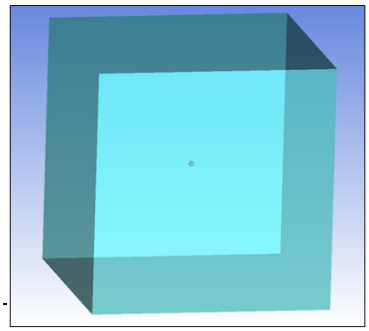

Fig. 2: CATIA 3D model of Heli-net for LLLR with payload

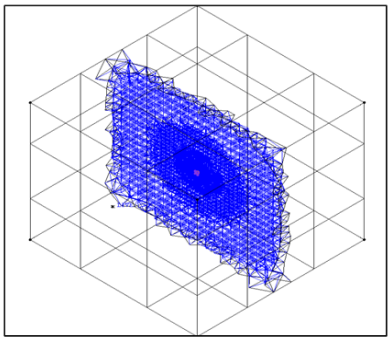

Fig. 3: A sectional view of tetrahedral mesh domain of Heli-net for LLLR

3. GOVERNING EQUATION AND NUMERICAL APPROACH

ANSYS FLUENT is used for CFD analysis. Flow is considered to be steady state, viscous, incompressible and turbulent. Forturbulent flows, the so called Reynolds Averaged Navier - Stokes (RANS) equations are used. They are derived from the Navier-Stokes equations.Here simulations are carried out with Realizable κ-εturbulent model with enhanced near wall treatment is used for turbulence modeling. Transport Equations for the Realizableκ-ε model are:

Here,
k = Turbulence kinetic energy

ε=Rate of dissipation

$$\frac{\partial}{\partial t}(\rho k)+\frac{\partial}{\partial x_i}(\rho k u_i)=\frac{\partial}{\partial x_j}\left[\left(\mu+\frac{\mu_t}{\sigma_k}\right)\frac{\partial k}{\partial x_j}\right]+G_k+G_b-\rho\epsilon-Y_M+S_k$$

$$\frac{\partial}{\partial t}(\rho\varepsilon)+\frac{\partial}{\partial x_j}(\rho\varepsilon u_j)=\frac{\partial}{\partial x_j}\left[\left(\mu+\frac{\mu_t}{\sigma_\varepsilon}\right)\frac{\partial\varepsilon}{\partial x_j}\right]+\rho C_1 S\varepsilon-\rho C_2\frac{\varepsilon^2}{k+\sqrt{\nu\epsilon}}+C_{1\varepsilon}\frac{\varepsilon}{k}C_{3\varepsilon}G_b+S_\varepsilon$$

Where,

$$C_1=max\left[0.43,\frac{\eta}{\eta+5}\right],\eta=S\frac{k}{\varepsilon},S=\sqrt{2S_{ij}S_{ij}}$$

- $G_k$represents the generation of turbulence kinetic energy due to the mean velocity gradients.
- G_b is the generation of turbulence kinetic energy due to buoyancy.
- Y_M represents the contribution of the fluctuating dilatation in compressible turbulence to the overall dissipation rate.
- $C_{1\varepsilon}$, $C_{2\varepsilon}$, and $C_{3\varepsilon}$ are constants. σ_k and σ_ε are the turbulent Prandtl numbers for κand ε, respectively.
- $S_k$andS_ε are user-defined source terms.

4. CFD ANALYSIS

Boundary conditions are defined for CFD simulation. All boundaries that represent the external walls represent the walls of the Helli-net are defined as 'Wall' boundary type. The 'Pressure far field' condition is applied to the outer boundary domain. Standard atmospheric pressure 0.1013 MPa and temperature 303.2 K is used for CFD analysis. For low subsonic flow, a density based, implicit, steady and absolute velocity formulation solver is considered. Helli-net is supposed to work as its wider length front manner. Reference areas are taken as that manner respectively. This is also proved during flight trial. Reference area A and length L has been taken as front C/s area of Helli-net and length of Helli-net for five different types of payloads condition respectively. Helli-net with Payload is like a bluff rectangular body. The grid check was performed and found satisfactory. Several iterations have been carried out to achieve convergence. The convergence criteria of 1E-05 are maintained with second order accuracy.

5. RESULTS AND DISCUSSION

Numerous aerodynamics coefficients and forces are generated after several CFD simulations at different windvelocities and angles of attack. Force in X direction increases with increase in wind velocity, but there are small changes with increase in

angle of attack. Fig. 4 shows the variation of C_D with angle of attack for payload1 case. Fig. 6 shows the comparison of drag coefficients for all payload conditions. Fig. 4,5, 6 and 7 follow the standard trend of $C_D$vs α and $C_L$vs α for all cases respectively. Drag coefficient increases with increase in negative angle of attack. With increase in negative angle of, C_L value increases first then decreases.

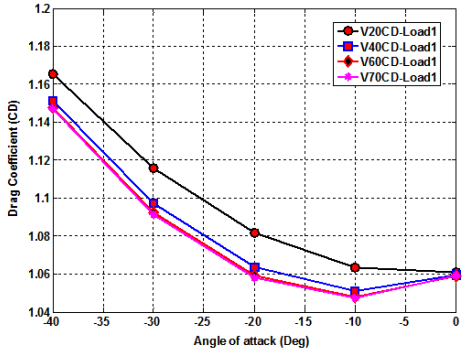

Fig. 4: Drag Coefficient vs Angle of attack (Degree) at various velocities for Load1

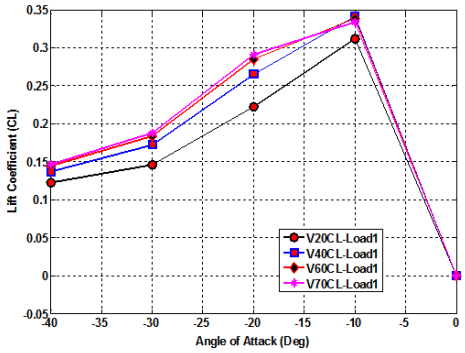

Fig. 5: Lift Coefficient vs Angle of attack (Degree) at various velocities for Load1

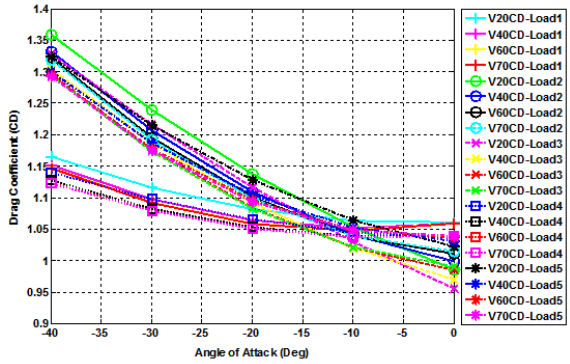

Fig. 6: Drag Coefficient vs Angle of attack (Degree) at various velocities and for different load conditions

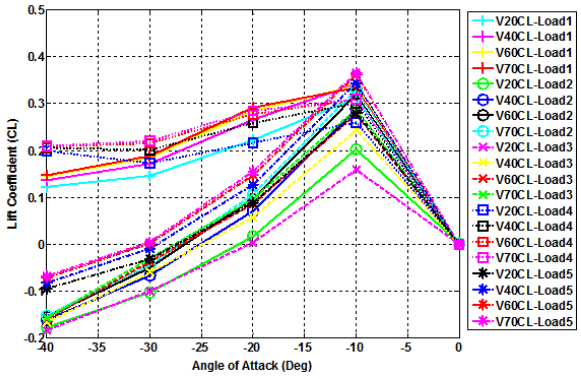

Fig. 7: Lift Coefficient vs Angle of attack (Degree) at various velocities and for different load conditions

There are fluctuations in the values of F_Z at different angles of attack. This is because of alternate formation and shedding of vortices that creates a regular change in pressure with consequent periodicity in side thrust on the payload. Fig. 10 shows the plot of force in Z direction with respect to angle of attack for payload1 and Fig. 8 shows the comparisons of forces in Z direction for all load conditions.

The computed flow fields obtained after CFD analysis for different velocities and various angles of attack have been plotted as contour plots and path line plots. Streamlines (path line) are used to visualize separations and re-attachments in the mean, in front of, on the top of, at the lateral sides and behind the payload.There is a horseshoe vortex [3] in front of the cube and recirculation regions on the top and behind the payload as shown in Fig. 9.For particular case for load2 at velocity 20knots and angle of attack 0º, front pressure is around 101391 Pascal and back pressure is around 101240 Pascal that is lower than front pressure. Pressure contour plot can be seen in Fig. 11 for load1 and angle of attack 0º. This gives rise to a significant value of the pressure drag, which is normally much higher than the friction drag.

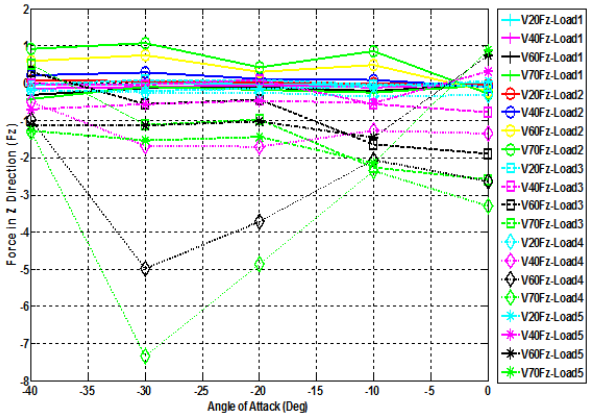

Fig. 8: A comparison of forces in Z direction at various velocities for different load conditions

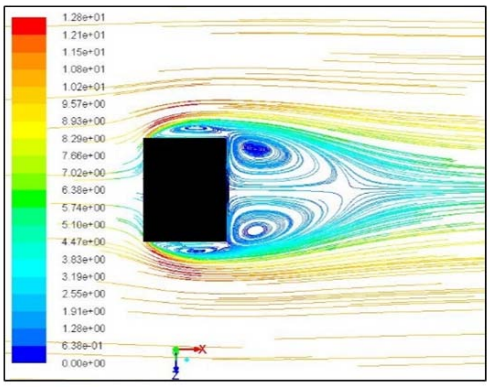

Fig. 9: Streamlines of the mean flow projected onto the center-plane of the payload

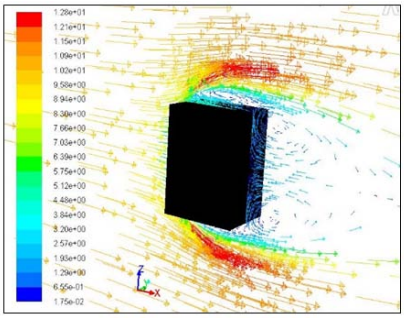

Fig. 10: Velocity vector colored by velocity magnitude (m/s) for load1 at 20K nots velocity and angle of attack 0º at Y = 0 plane

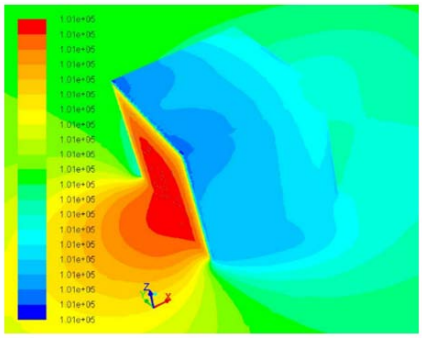

Fig. 11: Static pressure (Pascal) contour for L oad1at 20K nots velocity and angle of attack 0º

Fig. 12 to 16 show the velocity and pressure contours for different cases. A symmetric plane Z = 0, a sectional plane at X= 0.5 m and Y=0 m are created for clear visualization of flow behaviour. The computed flow fields obtained after CFD analysis for different velocities and various angles of attack have been plotted as contour plots.For typical case of V = 20 Knots and AOA = 0° for payload1, maximum velocity is 12.76307 m/s and minimum velocity is around zero at front part of the body that is stagnation velocity. Maximum pressure is exerted at the front part of the body that can be seen in Fig. 11.

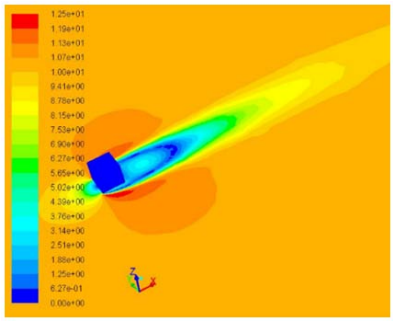

Fig. 12: Velocity magnitude (m/s) contour for load5 at velocity 70K nots and angle of attack -10º

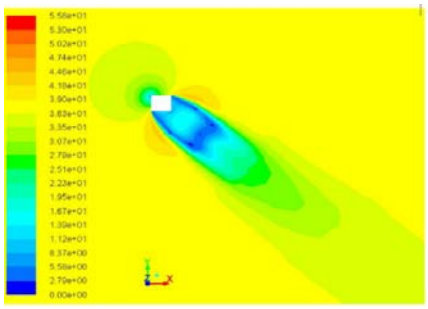

Fig. 13: Velocity magnitude (m/s) contours for load1at 20K nots velocity and angle of attack 0º

Consecutive high and low pressure regions are visible in pressure contour plots. This is to acquire the atmospheric pressure because of wake region has been created at the back of the payload [7].Due to change in angle of attack, Change in flow field is clearly visible in Fig. s 14 and 15.

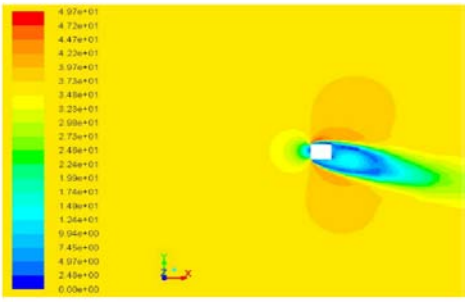

Fig. 14: Static pressure (Pascal) contour for load5 at velocity 70K nots and angle of attack -40º

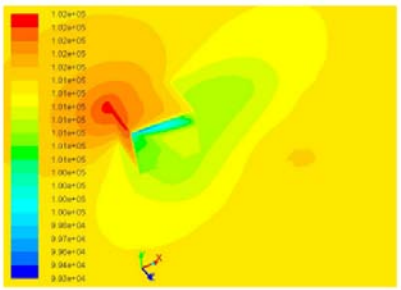

Fig. 15: Velocity magnitude (m/s) contour for load5 at velocity 70K nots and angle of attack -40º

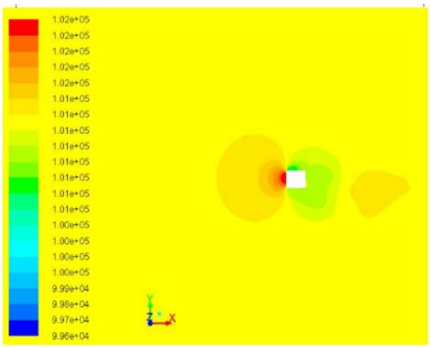

Fig. 16: Static pressure (Pascal) contour for load5 at velocity 70K nots and angle of attack -10°

6. CONCLUSIONS

Results from Computational fluid dynamics (CFD) Simulation are used for visualization of the flow around a three-dimensional bluff body that resembles Helli-net with payloads. Bluff bodies are a unique series of geometries in terms of flow dynamics. A weak region is created behind the body in all load conditions. The all payloads have flow separation due to pressure gradients. Separation causes pressure drag and therefore reduces the effectiveness of the body for producing lift. This CFD analysis showed how the pressure distribution and drag act around a bluff body. Result obtained after CFD analysis is compared with the standard data available for the bluff body. Drag coefficient obtained by CFD analysis compares well with drag coefficient data available in reference book by Dr.-Ing. S.F.Hoerner [1]. In simulation, the alternate low pressure and high-pressure regions have been noticed. This is to achieve atmospheric pressure by alternate compression and expansion. A horseshoe vortex is also seen in front of the cube and recirculation regions on the top and behind the payload. As it is the source of oscillating cross-flow forces that may induce significant oscillations of a structure if their frequency coincides with one of the natural frequencies of the structure.

7. ACKNOWLEDGEMENTS

We are thankful to Director ADRDE for allowing us to carry out research in this field. We also acknowledge the role of Heavy Drop Systems (HDS) group for providing necessary data for the analysis.

REFERENCES

[1] Dr.-Ing. S. F. Horner, "*Fluid dynamic drag*", published by the author, 1965.

[2] GrégoryTurbelin and René Jean Gibert "CFD calculations of indicial lift responses for bluff bodies" *Wind and Structures*, Vol. 4, No. 5 (2001) 0-00.

[3] Guido buresti "bluff-body aerodynamics" lecture notes of *International advanced school onwind-excited and aeroelastic vibrations of structures*,genoa, italy, june 12-16, 2000.

[4] KunihikoTaira†,William B. Dickson‡,TimColonius§, Michael H. Dickinson, Clarence W. Rowley "Unsteadiness in Flow over a Flat Plate at Angle-of-Attack at Low Reynolds Numbers" journal of *American Institute of Aeronautics and Astronautics.*

[5] S. Krajnovi´c1and L. Davidson "Flow Around a Three-dimensional Bluff body" *9th International Symposium on Flow Visualization*, Heriot-Watt University, Edinburgh, 2000.

[6] J. C. R. Hunt, C. J. Abell, J. A. Peterka, and H. Woo. "Kinematical studies of the flows around free or surface-mounted obstacles; applying topology to flow visualization". *Journal of Fluid Mechanics*, 86:179–200, 1978.

[7] PuneeshwarLalVerma, M. Govardhan, "Flow behind Bluff bodies in Side-by-Side Arrangement", *Journal of Engineering Science and Technology*, Vol. 6, No. 6 (2011) 745 – 768.

[8] Professor Fred Stern, "Bluff Body", published in 58:160 *Intermediate Fluid Mechanics*,2009.

[9] John D.Anderson,Jr, "*Fundamental of Aerodynamics*", published by the author, July, 2005.

[10] John D.Anderson,Jr, "*Computational Fluid Dynamics, the basics with application*", published by the author, 1995.